

Bound states of spin-orbit coupled cold atoms in a Dirac delta-function potential

Jieli Qin¹, Renfei Zheng², Lu Zhou^{2,3}

¹School of Physics and Electronic Engineering, Guangzhou University, 230 Wai Huan Xi Road, Guangzhou Higher Education Mega Center, Guangzhou 510006, China

²Department of Physics, School of Physics and Electronic Science, East China Normal University, Shanghai 200241, China

³Collaborative Innovation Center of Extreme Optics, Shanxi University, Taiyuan, Shanxi 030006, China

E-mail: lzhou@phy.ecnu.edu.cn

November 2019

Abstract. Dirac delta-function potential is widely studied in quantum mechanics because it usually can be exactly solved and at the same time is useful in modeling various physical systems. Here we study a system of delta-potential trapped spin-orbit coupled cold atoms. The spin-orbit coupled atomic matter wave has two kinds of evanescent modes, one of which has pure imaginary wavevector and is an ordinary evanescent wave; while the other with a complex number wave vector is recognized as oscillating evanescent wave. We identified the eigenenergy spectra and the existence of bound states in this system. The bound states can be constructed analytically using the two kinds of evanescent modes and we found that they exhibit typical features of stripe phase, separated phase or zero-momentum phase. In addition to that, the properties of semi-bound states are also discussed, which is a localized wave packet on a plane wave background.

Keywords: Spin-orbit coupling, cold atoms, Delta-function potential

Submitted to: *J. Phys. B: At. Mol. Phys.*

1. Introduction

Spin-orbit (SO) coupling has been widely studied in diverse branches of physics including nanotechnology [1, 2], nuclear physics [3, 4, 5], optics [7, 6, 8], condensed matter physics [9, 10] and cold atom physics [11, 12, 13]. For a charged particle with non-zero spin, its spin magnetic momentum will interact with the magnetic field induced by its movement, thus generating a coupling between its orbital motion and spin degree of freedom. For neutral cold atom systems, SO-coupling can be artificially generated via

a Raman coupling scheme [14]. The occurrence of SO-coupling will greatly enrich the physics of atomic matter wave [15, 16, 12]. Many emergent phenomena such as spin Hall effect [17], topological insulator [18], Zitterbewegung [19, 20, 21, 22], supersolid [23, 24, 25, 26], solitons [27, 28, 29, 30], Beliaev damping [31] and spin-dependent atom optics [32, 33, 34, 35, 36, 37, 38, 39, 40, 41, 42, 43] have been reported.

It was found that in the presence of SO-coupling the atomic system can display a rich phase diagram in which the ground state wavefunction can favor stripe, spin separated or zero momentum phase [14, 44, 45, 46, 47]. Specifically, the stripe phase can be regarded as a signature of supersolid [23, 24, 25, 26] which receives much recent attention. Physical insight into the properties of eigenfunction of the SO-coupled ultracold atoms can be gained via bound state solutions. Previous work has solved bound state in a one-dimensional short-range potential, and predicts a type of spin-orbitinduced extra states [48]. More interestingly, bound state in the continuum can exist under appropriate trapping potentials [49].

In this article we analytically study the bound states of SO-coupled atomic matterwave in a δ -function potential. Physical models with δ -function potential play significant roles in quantum mechanics. Analytical or partially analytical solutions can be deduced for these models and in the meanwhile they provide physical insight into real systems. Typical examples include the Kronig-Penney model with δ -function potential [50], the hydrogen-like atoms and diatomic molecules [51], the inter-atom interaction in ultra cold atomic cloud [52, 53], very narrow potential [54, 55, 56, 57], obstacle [58, 59] and impurity [60, 61]. It is well known that a δ -function potential well supports only one bound state which is constructed with free particle evanescent waves. For SO-coupled matter wave, there are three different types of free particle modes: plane wave, ordinary evanescent wave and oscillating evanescent waves [63, 36]. We found that there exist two types of bound states which can be constructed using the oscillating evanescent and ordinary evanescent waves, respectively. The bound state constructed with oscillating evanescent waves has stripe structure on its density profile, while the bound state with ordinary evanescent waves is a zero momentum wave packet. Due to the spin-1/2 nature of the system, a δ -function potential well can (but not always) support bound states both in ground state and excited state. A separated phase bound state can then be constructed by superposing the ground and excited bound state. Besides these bound states, we found that there also exists a kind of semi-bound state, which is a localized state on a plane wave background. The interference between the localized state and the plane wave background will produce a dip (bump) on the density profile for a δ -potential well (barrier).

2. Model and eigensolution of free SO-coupled cold atomic matter wave

As schematically shown in figure 1, we consider a system of quasi-one-dimensional SO-coupled cold atoms subjected to a spin-independent δ -function potential. The SO coupling is realized by a typical Raman scattering scheme [14]. And the spin-

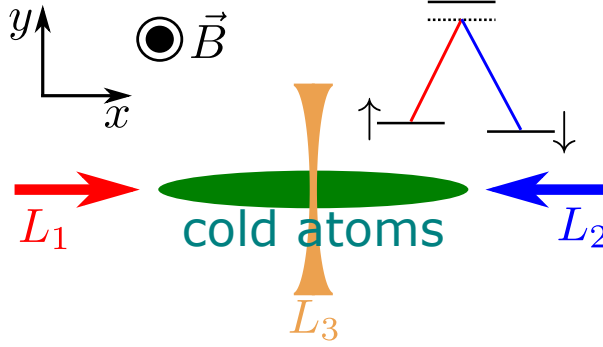


Figure 1. Schematic of the considered system. A quasi-one-dimensional spinor cold atomic cloud (two Zeeman levels acts as the pseudo-spin states) is shined by two x -direction counterpropagating laser beams (L_1 and L_2) to realize the SO-coupling [14]. A third far off-resonant tightly focused laser beam (L_3) shining from y -direction generates a spin-independent delta-function potential [54, 55].

independent δ -potential is generated by a far off-resonant laser beam [62] which is tightly focused at the center of the atomic cloud [54, 55]. Such a system can be described by the Hamiltonian

$$H = H_0 - V_0 \delta(x), \quad (1)$$

with V_0 being the depth of δ -function potential, and H_0 being the free particle Hamiltonian of SO-coupled matter wave

$$H_0 = \begin{pmatrix} \frac{\hbar^2}{2m} (k_x - k_c)^2 & \hbar\Omega/2 \\ \hbar\Omega/2 & \frac{\hbar^2}{2m} (k_x + k_c)^2 \end{pmatrix}, \quad (2)$$

which can be implemented with a Raman coupling scheme in cold atom system [14]. Here \hbar is the reduced Planck constant, m is the mass of an atom, $p_x = \hbar k_x = -i\hbar\partial/\partial x$ is the x -direction momentum operator, k_c signals SO-coupling strength and Ω is the Rabi coupling strength. For simplicity, we have assumed that the interatomic collision interaction is eliminated using the technique of Feshbach resonance [64, 65].

Since the total Hamiltonian H equals H_0 except at the point $x = 0$, we first give a brief discussion on the properties of free particle Hamiltonian H_0 . The eigenenergy E of H_0 is given by the equation

$$\left[E - \frac{\hbar^2 (k_x^2 + k_c^2)}{2m} \right]^2 - \left(\frac{\hbar^2 k_c k_x}{m} \right)^2 - \left(\frac{\hbar\Omega}{2} \right)^2 = 0. \quad (3)$$

For a given energy E , this quartic algebraic equation has four solutions

$$k_x = \pm \sqrt{k_c^2 + \frac{2mE}{\hbar^2}} \pm \frac{\sqrt{8mEk_c^2 + m^2\Omega^2}}{\hbar}. \quad (4)$$

These four solutions can generally be written as $k_x = \beta + i\alpha$, with α and β being two real numbers. In the wavefunction $e^{ik_x x} = e^{-\alpha x} e^{i\beta x}$, the real part β of wavevector k_x contributes a plane wave factor, while the imaginary part α contributes an exponential decay factor. Thus, depending on the values of α and β , the corresponding free particle

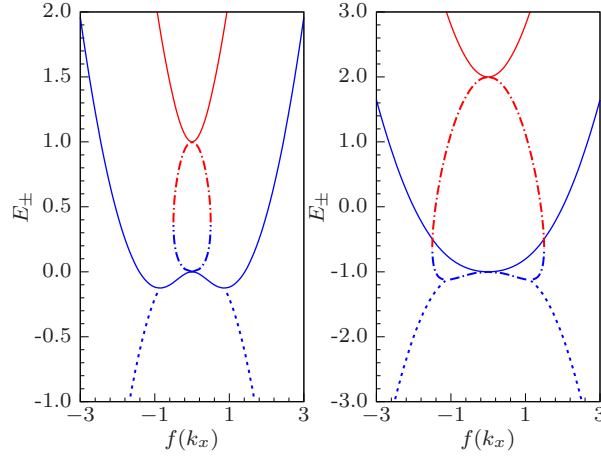


Figure 2. Free particle energy spectra of SO-coupled atomic matter waves. Left panel: strong SO-coupling case with parameters $k_c^2 > m^2 \Omega^2 / (4\hbar)$ ($k_c = 1, \Omega = 1$). Right panel: weak SO-coupling case with parameters $k_c^2 < m^2 \Omega^2 / (4\hbar)$ ($k_c = 1, \Omega = 3$). The upper branch spectrum E_+ is plotted in red color, while the lower branch E_- is plotted in blue color. The plane, ordinary evanescent and oscillating evanescent wave modes are plotted with solid, dash-dot and dash lines respectively. For plane wave mode, k_x is a real number, x -axis is simply set to $f(k_x) = k_x$; for ordinary evanescent wave mode, k_x has no real part, x -axis is set to its imaginary part $f(k_x) = \text{Im}(k_x)$; and for oscillating evanescent wave mode, $k_x = \pm\beta \pm i\alpha$ is a complex number, x -axis is set to $f(k_x) = \text{sgn}[\text{Im}(k_x)] \cdot |k_x|$ (note that in such a way the points for $+\beta$ and $-\beta$ will overlap with each other, thus the seemingly two curves in the figure are in fact four curves). Other parameters used are $m = \hbar = 1$.

waves can be divided into three types: (1) Plane wave with $\alpha = 0, \beta \neq 0$; (2) Ordinary evanescent wave with $\alpha \neq 0, \beta = 0$; and (3) Oscillating evanescent wave when $\alpha, \beta \neq 0$.

From equation (3), eigenenergy can be further split into two spectrum branches (referred as upper and lower branch)

$$E_{\pm}(k_x) = \frac{\hbar^2(k_x^2 + k_c^2)}{2m} \pm \sqrt{\left(\frac{\hbar^2 k_c k_x}{m}\right)^2 + \left(\frac{\hbar\Omega}{2}\right)^2}, \quad (5)$$

with the corresponding eigenstates

$$\Psi_{\pm} = \chi_{\pm}(k_x) e^{ik_x x} = C_{\pm} \begin{pmatrix} \zeta_{\pm} \\ 1 \end{pmatrix} e^{ik_x x}, \quad (6)$$

in which $\zeta_{\pm} = -\left(2\hbar k_c k_x \mp \sqrt{4\hbar^2 k_c^2 k_x^2 + m^2 \Omega^2}\right) / m\Omega$ and $C_{\pm} = 1/\sqrt{1 + |\zeta_{\pm}|^2}$ is the normalization constant.

Equation (4) indicates that there are four states for any energy E , the eigenenergy dispersion display two typically different structures depending on the SO-coupling strength:

(i) The strong SO-coupling case with $k_c^2 > m^2 \Omega^2 / 4\hbar$. In this case, when $E > E_+(0) = \hbar^2 k_c^2 / 2m + \hbar\Omega/2$, both the upper and lower branches support two plane wave states with k_x real. In the region $E \in [E_-(0) = \hbar^2 k_c^2 / 2m - \hbar\Omega/2, E_+(0)]$,

Energy range	Strong coupling						Weak coupling					
	P		Ev		OE		P		Ev		OE	
	U	L	U	L	U	L	U	L	U	L	U	L
$[E_+(0), +\infty]$	2	2					2	2				
$[E_-(i\alpha_0), E_+(0)]$		2	2					2	2			
$[E_-(0), E_-(i\alpha_0)]$		2		2				2		2		
$[E_-(k_0), E_-(0)]$		4								4		
$[-\infty, E_-(k_0)]$						4						4

Table 1. Plane (P), ordinary evanescent (Ev), and oscillating evanescent (OE) mode numbers of SO-coupled atomic matter wave in different energy ranges. Strong coupling means $k_c^2 > m^2\Omega^2/(4\hbar)$, while weak coupling means $k_c^2 < m^2\Omega^2/(4\hbar)$. Letters “U” and “L” are used to label the upper and lower branch of the spectrum. In the table α_0 and k_0 are $\alpha_0 = m\Omega/(2\hbar k_c)$, $k_0 = \sqrt{k_c^2 - m^2\Omega^2/(4\hbar^2 k_c^2)}$. The expression of function E_{\pm} is given by formulae (5) in the text.

there are two plane wave states in the lower spectrum branch while the other two are ordinary evanescent states coming from either the upper branch when $E > E_-(i\alpha_0) = (4\hbar^2 k_c^4 - m^2\Omega^2)/8mk_c^2$ ($\alpha_0 = m\Omega/2\hbar k_c$) or lower branch when $E < E_-(i\alpha_0)$. For $E \in [E_-(k_0) = -m\Omega^2/8k_c^2, E_-(0)]$ with $k_0 = \sqrt{k_c^2 - m^2\Omega^2/(4\hbar^2 k_c^2)}$ there are four plane wave states in the lower branch. Four oscillating evanescent states possess minimum energies with $E < E_-(k_0)$ and they are linked to the energy minimum of the upper energy spectra at the points $|k_x| = k_0$.

(ii) The weak SO-coupling case with $k_c^2 < m^2\Omega^2/4\hbar$. It differs from the strong coupling case only in the energy region $[E_-(k_0), E_-(0)]$, in which all four eigenstates come from the lower branch are ordinary evanescent waves with k_x imaginary.

In order to better understand the properties of these eigenstates, we plot in figure 2 the energy spectra as a function of k_x for $k_c = 1$ and two typical values of Ω , signaling the strong coupling and weak coupling case respectively. The corresponding numbers of plane, evanescent and oscillating evanescent modes in different energy ranges are also summarized in Table 1.

3. Bound states and semi-bound states with delta-function potential

The bound state of a δ -function potential well $V(x) = -V_0\delta(x)$ can be constructed using the free particle modes by matching the boundary conditions at $x = 0$. Because the plane wave mode extends to infinity, it can not be used to construct a bound state. While ordinary and oscillating evanescent wave modes decay to zero when x approaches $+\infty$ or $-\infty$, they are the candidates for bound state constructing. So based on the discussion in section 2, it is concluded that bound states can exist in energy range $[-\infty, E_-(k_0)]$

for both strong and weak SO-coupling, and in energy range $[E_-(k_0), E_-(0)]$ for only weak SO-coupling, since in these energy ranges there exist the candidate modes. And in energy range $[E_-(0), E_+(0)]$, the plane wave and ordinary evanescent wave modes exist simultaneously, this gives a chance to construct a kind of semi-bound state, which shows as a localized wave packet on plane wave background. These states will be discussed in the rest content of this section one by one.

In the energy range $E < E_-(k_0)$, as having been discussed above there exist four oscillating evanescent modes and bound states can be constructed using them. One can find that the wave vector (4) of these four modes have symmetrical form $k_x = \pm\beta \pm i\alpha$ and we label them as $k_1 = \beta + i\alpha$, $k_2 = -\beta + i\alpha$, $k_3 = \beta - i\alpha$, $k_4 = -\beta - i\alpha$, so the bound state can be written as

$$\Psi_b = \begin{cases} [A_1\chi_-(k_1)e^{i\beta x} + A_2\chi_-(k_2)e^{-i\beta x}]e^{-\alpha x}, & x > 0, \\ [A_3\chi_-(k_3)e^{i\beta x} + A_4\chi_-(k_4)e^{-i\beta x}]e^{\alpha x}, & x < 0, \end{cases} \quad (7)$$

with A_1, A_2, A_3, A_4 and eigenenergy E (note that $k_{1,2,3,4}$ are determined by E according to formula (4)) to be determined by normalization constraint

$$\int_{-\infty}^{\infty} |\Psi_b(x)|^2 dx = 1, \quad (8)$$

and boundary conditions at $x = 0$: continuity of the wave function

$$\Psi_b|_{0+} = \Psi_b|_{0-}, \quad (9)$$

with

$$\Psi_b|_{0+} = A_1\chi_-(k_1) + A_2\chi_-(k_2), \quad (10)$$

$$\Psi_b|_{0-} = A_3\chi_-(k_3) + A_4\chi_-(k_4), \quad (11)$$

and jump of the first-order derivation caused by divergence of δ -function potential

$$\left. \frac{\partial \Psi_b}{\partial x} \right|_{0+} - \left. \frac{\partial \Psi_b}{\partial x} \right|_{0-} = -\frac{2mV_0}{\hbar^2} \Psi_b(x=0), \quad (12)$$

with

$$\left. \frac{\partial \Psi_b}{\partial x} \right|_{0+} = ik_1 A_1\chi_-(k_1) + ik_2 A_2\chi_-(k_2), \quad (13)$$

$$\left. \frac{\partial \Psi_b}{\partial x} \right|_{0-} = ik_3 A_3\chi_-(k_3) + ik_4 A_4\chi_-(k_4). \quad (14)$$

Solving equations (9) and (12), one can have two solutions (the lower energy one is the ground state and the other one is an excited state) fulfill properties $|A_1| = |A_2| = |A_3| = |A_4|$, indicating that the bound state is a spin symmetric state with $|\Psi_{b,\uparrow}|^2 = |\Psi_{b,\downarrow}|^2$. From equation (7) one can understand that the interference between $e^{i\beta x}$ and $e^{-i\beta x}$ terms will produce an interference stripe on the density profile of bound states. This type of bound state has very similar properties as the stripe phase state in free space or harmonically trapped SO-coupled matter wave [46]. In figure 3, examples of such bound states are plotted for parameters $V_0 = 0.1$, $k_c = 1$, $\Omega = 1$, clearly

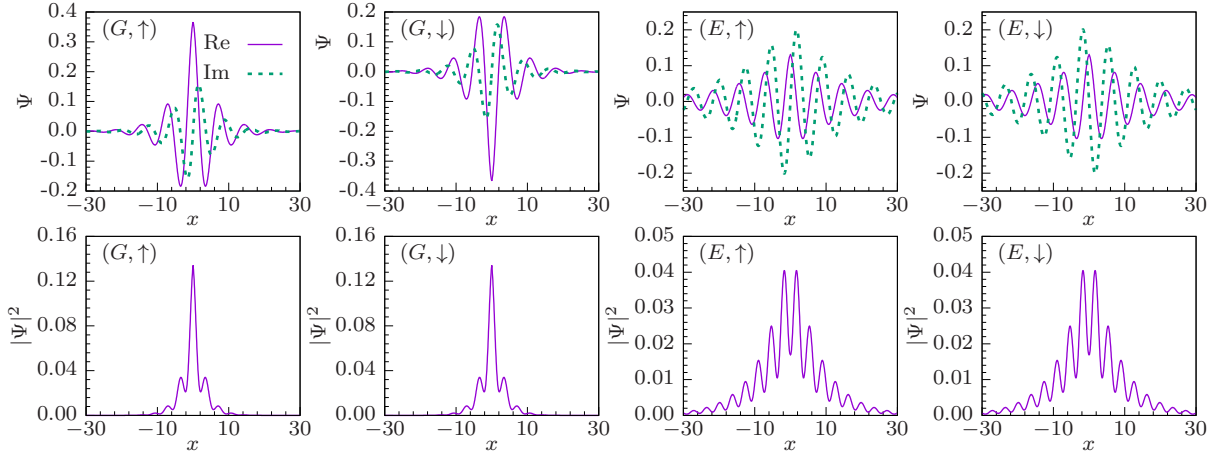


Figure 3. Oscillating evanescent wave bound states. Ground (“G”) and Excited (“E”) states of SO-coupled matter wave in δ -function potential well are plotted for parameters $V_0 = 0.1, k_c = 1, \Omega = 1$. Top panels are real (solid) and imaginary (dashed) parts of the wave function Ψ with different spins (labeled with “ \uparrow ” and “ \downarrow ”). Bottom panels are the corresponding densities $|\Psi|^2$. The energies of the ground and excited states are -0.1391 and -0.1267 respectively. Natural unit $m = \hbar = 1$ is applied.

demonstrating spin mixed stripe phase structure. We also note that no-node theorem does not hold here because of SO-coupling [66, 67].

The bound states can also be constructed via the linear superposition of the ground and excited states. In figure 4, the superposition state $\Psi_{b,G+E} = (\Psi_{b,G} + \Psi_{b,E})/\sqrt{2}$ is plotted which is a spin- \uparrow component dominated state. Similarly a spin- \downarrow component dominated state can also be constructed by superposing $\Psi_{b,G}$ and $\Psi_{b,E}$ with opposite phase $\Psi_{b,G-E} = (\Psi_{b,G} - \Psi_{b,E})/\sqrt{2}$. This resembles the separated phase discussed in [46] with nonzero spin polarization. But, it should be noted that because the ground and excited states have different eigenenergies, these superposition states are not stationary states of the system.

The bound states can also exist in the energy region $[E_-(k_0), E_-(0)]$ for a weak SO-coupling ($k_c^2 < m^2\Omega^2/(4\hbar)$). In such a case, there exist four ordinary evanescent modes for a given energy E , the corresponding wavevectors (4) are pure imaginary and have form $k_{1,3} = \pm i\kappa_1, k_{2,4} = \pm i\kappa_2$. The bound state can then be written in the following form

$$\Psi_b = \begin{cases} A_1 \chi_-(k_1) e^{-\kappa_1 x} + A_2 \chi_-(k_2) e^{-\kappa_2 x}, & x > 0, \\ A_3 \chi_-(k_3) e^{\kappa_1 x} + A_4 \chi_-(k_4) e^{\kappa_2 x}, & x < 0, \end{cases} \quad (15)$$

which decays exponentially and is very similar to the bound states in the SO-uncoupled case. Applying the boundary conditions and normalization constraints (similar to equaitons (8, 9, 12)) one can solve the bound states. An example is given in figure 5, the bound state is spin symmetric and can be viewed as the “zero momentum” states discussed in [46].

We also examined the spectrum with δ -function potential well. In the top two and bottom left panels of figure 6, the binding energies of the ground and excited

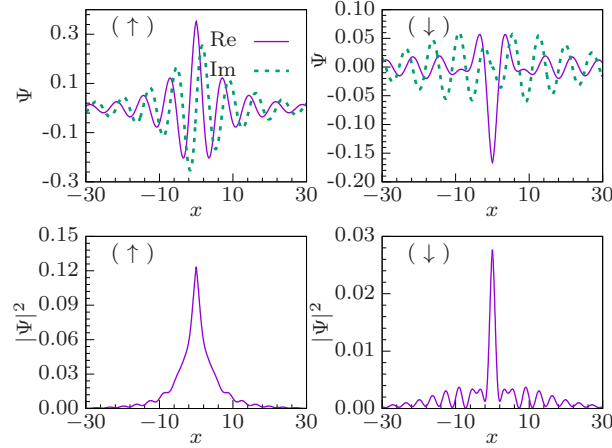


Figure 4. Separated phase bound state as a superposition of ground and excited states, $(\Psi_{b,G} + \Psi_{b,E})/\sqrt{2}$. Top panels are the real (solid) and imaginary (dashed) parts of the spin- \uparrow and spin- \downarrow wave functions. Bottom panels are the corresponding densities $|\Psi|^2$. Parameters are the same as in figure 3.

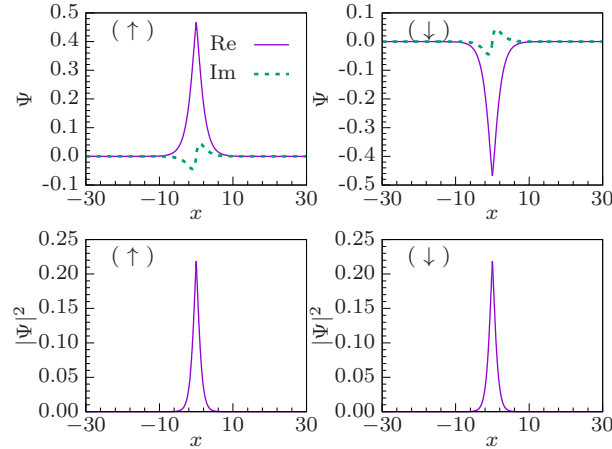


Figure 5. Ordinary evanescent wave bound state. Ground state of SO-coupled matter wave in δ -function potential well is plotted for parameters $V_0 = 0.25, k_c = 1, \Omega = 3$. Top panels are the real (solid) and imaginary (dashed) parts of the spin- \uparrow and spin- \downarrow wave functions. Bottom panels are the corresponding densities $|\Psi|^2$. The energy of this state is -1.0625 . Natural unit $m = \hbar = 1$ is applied.

bound states are plotted as a function of δ -function potential well depth V_0 for Rabi coupling strength $\Omega = 0, 1$ and 3 . When $\Omega = 0$, the two spin components are not coupled with each other, each component can be separately treated as a usual δ -function potential problem (except that the momentum is shifted by $\pm \hbar k_c$), thus there exist two bound states with degenerate energy $E_{b,G} = E_{b,E} = -mV_0^2/(2\hbar^2)$. When $\Omega \neq 0$, this degeneracy is eliminated. For a small value of $\Omega = 1$ (or in other words, a strong SO-coupling since $k_c^2 > m^2\Omega^2/4\hbar$ is fulfilled), both the ground and excited states can exist regardless of the value of V_0 . Even when $V_0 \rightarrow 0$ (approaching the free particle limit), the system has two solutions corresponding to the two minimums of the lower dispersion branch. However, for a large value of $\Omega = 3$ (weak SO-coupling since $k_c^2 < m^2\Omega^2/4\hbar$),

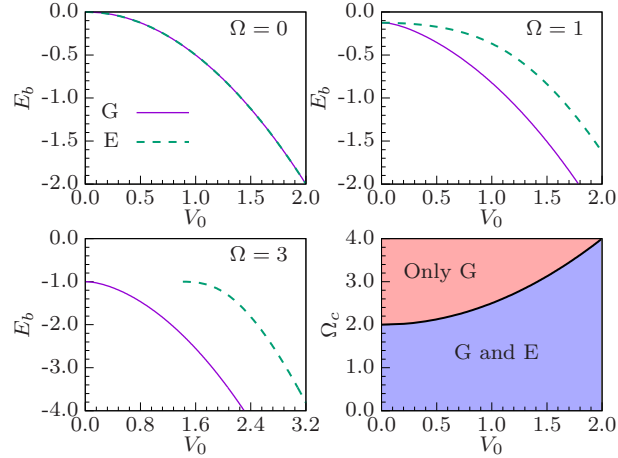


Figure 6. δ -function potential well bounded spectrum. The binding energies of the ground (“G”) and excited (“E”) states are plotted as a function of potential well depth V_0 for parameters $\Omega = 0, 1, 3$ in the top two and bottom left panels respectively. In the bottom right panel, the critical value of Rabi coupling Ω_c for the disappearing of the excited state is plotted as a function of potential well depth V_0 , the solid black line. Below this line, in the light blue color filled area, there exist both the ground and excited states. While, above this line, in the light red color filled area, only the ground state can exist. In all the panels, SO-coupling strength is set to $k_c = 1$ and natural unit $m = \hbar = 1$ is applied.

the excited state can be lifted so high that a shallow potential well can no longer trap it. Thus, we see that for V_0 smaller than a critical value, the excited state disappears. This also coincides with the fact that for weak SO-coupling the lower dispersion branch of the free particle spectrum only has one minimum. And in the bottom right panel, we show the critical value of Rabi coupling strength Ω_c for the disappearing of the excited state as a function of V_0 , see the solid black line. Below this critical line, both the ground and excited states can exist. While above this line, the potential well can no longer support an excited bound state, only the ground state can exist. In this panel, we also noticed that when $V_0 \rightarrow 0$, the critical Rabi coupling $\Omega_c \rightarrow 2$ which is just the demarcation point between strong and weak SO-coupling strength ($\sqrt{4\hbar k_c^2/m^2} = 2$). This also agrees with the above free particle limit discussion.

In the energy region $[E_-(0), E_+(0)]$, for a given energy E there are two ordinary evanescent modes and two plane wave modes, the corresponding wavevectors (4) have form $k_{1,3} = \pm i\kappa$ and $k_{2,4} = \pm k$. One can then construct a semi-bound state as follows

$$\Psi_{sb} = \Psi_P + \Psi_E, \quad (16)$$

where Ψ_P is a plane wave background consisting of incident, transmission and reflection waves (their amplitudes are 1, t , r respectively)

$$\Psi_P = \begin{cases} t\chi_-(k_2)e^{ikx}, & x > 0, \\ \chi_-(k_2)e^{ikx} + r\chi_-(k_4)e^{-ikx}, & x < 0, \end{cases} \quad (17)$$

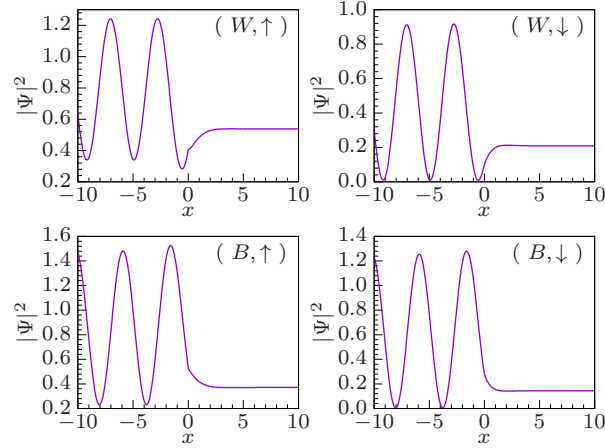


Figure 7. Semi-bound states of SO-coupled matter wave in δ -function potential well (“W”, top panels) and barrier (“B”, bottom panels). Density profiles of spin- \uparrow and spin- \downarrow components are plotted. Parameters used are $E_0 = -0.9$, $V_0 = \pm 0.25$ ($+0.25$ for a potential well, while -0.25 for a potential barrier), $k_c = 1$, $\Omega = 3$ and $m = \hbar = 1$.

and Ψ_E is a localized wave packet constructed using the two ordinary evanescent modes

$$\Psi_E = \begin{cases} A_1 \chi_{\pm}(k_1) e^{-\kappa x}, & x > 0, \\ A_3 \chi_{\pm}(k_3) e^{\kappa x}, & x < 0. \end{cases} \quad (18)$$

Here t, r and A_1, A_3 are parameters to be determined by boundary conditions. We note that such a semi-bound state is actually a scattering state, thus it can not only exist for a δ -potential well but also a δ -potential barrier. In figure 7, examples of such semi-bound states are shown for parameters $k_c = 1, \Omega = 3$ and $V_0 = \pm 0.25$ ($+0.25$ for a potential well, while -0.25 for a potential barrier). The density profiles of both spin components are plotted in this figure. In the left-half space ($x < 0$), the interference between incident and reflected waves produces an interference fringe. In the right-half space ($x > 0$), the transmission wave produces a flat density background. And around the location of δ -potential ($x = 0$), a dip of density on plane wave ground can be observed for a potential well, while a bump is observed for a potential barrier. This semi-bound state represents the coupling between the bound state and the plane wave propagating state, thus bound states in the continuum don’t exist in the present single-particle system [68].

4. Summary

In summary, we studied the bound and semi-bound states of SO-coupled matter wave in a δ -function potential. We found that there are two kinds of bound state in the system, one of which is a stripe one constructed using oscillating evanescent wave, while the other one constructed using ordinary evanescent wave is an ordinary one having the similar feature as the SO-uncoupled case. For SO-coupled matter wave, a δ -potential well can (but not always) support both a ground and an excited bound state. By superposing these two states, a separated phase state can also be constructed. Besides the bound

states, there also exists a kind of semi-bound state (a localized wave packet on a plane wave background). For a δ -function potential well, a dip emerges on the plane wave background. While for a δ -function potential barrier, a bump is formed on the plane wave background.

Acknowledgments

This work is supported by the National Natural Science Foundation of China (Grant Nos. 11904063, 11847059, 11374003, and 11574086).

References

- [1] Majumdar S, Majumdar H S and Österbacka R 2011 Organic spintronics *Comprehensive nanoscience and technology* ed D Andrews, G Scholes and G Wiederrecht (Academic Press) pp 109-142
- [2] Tan S G and Jalil M B A 2012 Spintronics and spin Hall effects in nanoelectronics *Introduction to physics of nanoelectronics* ed S G Tan and M Jalil (Woodhead) pp 141-197
- [3] Hope J 1957 Nuclear spin-orbit energy for oscillator wave functions *Phys. Rev.* **106**, 771
- [4] Bell J S and Skyrme T H R 1994 CVIII: The nuclear spin-orbit coupling *Selected papers with commentary of Tony Hilton Royle Skyrme* ed G E Brown (World Scientific) pp 71-84
- [5] Kaiser N 2007 Σ -nuclear spin-orbit coupling from two-pion exchange *Phys. Rev. C* **76**, 068201
- [6] Cardano F and Marrucci L 2015 Spin-orbit photonics *Nat. Photonics* **9**, 776
- [7] Bliokh K Y, Rodríguez-Fortuño F J, Nori F and Zayats A V 2015 Spin-orbit interactions of light *Nat. Photonics* **9**, 796
- [8] Sala V G, Solnyshkov D D, Carusotto I, Jacqmin T, Lemaître A, Terças H, Nalitov A, Abbarchi M, Galopin E, Sagnes I, Bloch J, Malpuech G and Amo A 2015 Spin-orbit coupling for photons and polaritons in microstructures *Phys. Rev. X* **5**, 011034
- [9] Bihlmayer G, Rader O and Winkler R 2015 Focus on the Rashba effect *New J. Phys.* **17** 050202
- [10] Rashba E I 2016 Spin-orbit coupling goes global *J. Phys. Condens. Matter* **28** 421004
- [11] Galitski V and Spielman I B 2013 Spin-orbit coupling in quantum gases *Nature* **494** 49
- [12] Zhai H 2015 Degenerate quantum gases with spin-orbit coupling: a review *Reports Prog. Phys.* **78** 026001
- [13] Zhang Y, Mossman M E, Busch T, Engels P and Zhang C 2016 Properties of spin-orbit-coupled Bose-Einstein condensates *Front. Phys.* **11** 118103
- [14] Lin Y-J, Jimenez-Garcia K and Spielman I B 2011 Spin-orbit-coupled Bose-Einstein condensates *Nature* **471** 83
- [15] Dalibard J, Gerbier F, Juzeliū G and Öhberg P 2011 Colloquium: Artificial gauge potentials for neutral atoms *Rev. Mod. Phys.* **83** 1523
- [16] Goldman N, Juzeliūnas G, Öhberg P and Spielman I B 2014 Light-induced gauge fields for ultracold atoms *Reports Prog. Phys.* **77** 126401
- [17] Sinova J, Valenzuela S O, Wunderlich J, Back C H and Jungwirth T 2015 Spin Hall effects *Rev. Mod. Phys.* **87** 1213
- [18] Hasan M Z and Kane C L 2010 Colloquium: Topological insulators *Rev. Mod. Phys.* **82** 3045
- [19] Schrödinger E 1930 Über die kräftefreie bewegung in der relativistischen quantenmechanik *Sitzungsber. Preuss. Akad. Wiss. Phys. Math. Kl.* **24**, 418
- [20] Hestenes D 2010 Zitterbewegung in quantum mechanics *Found. Phys.* **40** 1
- [21] LeBlanc L J, Beeler M C, Jiménez-García K, Perry A R, Sugawa S, Williams R A and Spielman I B 2013 Direct observation of Zitterbewegung in a Bose-Einstein condensate *New J. Phys.* **15** 073011

- [22] Qu C, Hamner C, Gong M, Zhang C and Engels P 2013 Observation of Zitterbewegung in a spin-orbit-coupled Bose-Einstein condensate *Phys. Rev. A* **88** 021604
- [23] Li J-R, Lee J, Huang W, Burchesky S, Shteynas B, Top F Ç, Jamison A O and Ketterle W 2017 A stripe phase with supersolid properties in spin-orbit-coupled Bose-Einstein condensates *Nature* **543** 91
- [24] Wang J-G and Yang S-J 2017 Supersolid phases in Bose gases with three-dimensional spin-orbit coupling *J. Phys. B At. Mol. Opt. Phys.* **50** 135001
- [25] Liao R 2018 Searching for supersolidity in ultracold atomic Bose condensates with Rashba spin-orbit coupling *Phys. Rev. Lett.* **120** 140403
- [26] Zhu C, Chen L, Hu H, Liu X-J and Pu H 2019 Spin-exchange-induced exotic superfluids in a Bose-Fermi spinor mixture *Phys. Rev. A* **100** 031602
- [27] Achilleos V, Frantzeskakis D J, Kevrekidis P G and Pelinovsky D E 2013 Matter-wave bright solitons in spin-orbit coupled Bose-Einstein condensates *Phys. Rev. Lett.* **110** 264101
- [28] Xu Y, Zhang Y and Wu B 2013 Bright solitons in spin-orbit-coupled Bose-Einstein condensates *Phys. Rev. A* **87** 013614
- [29] Zhang Y C, Zhou Z W, Malomed B A and Pu H 2015 Stable solitons in three dimensional free space without the ground state: self-trapped Bose-Einstein condensates with spin-orbit coupling *Phys. Rev. Lett.* **115** 253902
- [30] Zhu X, Li H, Shi Z, Xiang Y and He Y 2017 Gap solitons in spin-orbit-coupled Bose-Einstein condensates in mixed linear-nonlinear optical lattices *J. Phys. B At. Mol. Opt. Phys.* **50** 155004
- [31] Wu R and Liang Z 2018 Beliaev damping of a spin-orbit-coupled Bose-Einstein condensate *Phys. Rev. Lett.* **121** 180401
- [32] Jacob A, Öhberg P, Juzeliūnas G and Santos L 2007 Cold atom dynamics in non-Abelian gauge fields *Appl. Phys. B* **89** 439
- [33] Juzeliūnas G, Ruseckas J, Jacob A, Santos L and Öhberg P 2008 Double and negative reflection of cold atoms in non-Abelian gauge potentials *Phys. Rev. Lett.* **100** 200405
- [34] Juzeliūnas G, Ruseckas J, Lindberg M, Santos L and Öhberg P 2008 Quasirelativistic behavior of cold atoms in light fields *Phys. Rev. A* **77** 011802
- [35] Zhou L, Pu H and Zhang W 2013 Anderson localization of cold atomic gases with effective spin-orbit interaction in a quasiperiodic optical lattice *Phys. Rev. A* **87** 023625
- [36] Zhou L, Qin J-L, Lan Z, Dong G and Zhang W 2015 Goos-Hänchen shifts in spin-orbit-coupled cold atoms *Phys. Rev. A* **91** 031603
- [37] Zhou L, Zheng R-F and Zhang W 2016 Spin-sensitive atom mirror via spin-orbit interaction *Phys. Rev. A* **94** 053630
- [38] Kartashov Y V, Konotop V V, Zezyulin D A and Torner L 2016 Bloch oscillations in optical and Zeeman lattices in the presence of spin-orbit coupling *Phys. Rev. Lett.* **117** 215301
- [39] Kumar R and Ghosh S 2018 Entanglement-like properties in spin-orbit coupled ultra cold atom and violation of Bell-like inequality *J. Phys. B At. Mol. Opt. Phys.* **51** 165301
- [40] Zhang Y, Gui Z and Chen Y 2019 Nonlinear dynamics of a spin-orbit-coupled Bose-Einstein condensate *Phys. Rev. A* **99** 023616
- [41] Qin J 2019 Effect of spin-orbit coupling on tunnelling escape of Bose-Einstein condensate *J. Phys. B At. Mol. Opt. Phys.* **52** 045002
- [42] Ji W, Zhang K, Zhang W and Zhou L 2019 Bloch oscillations of spin-orbit-coupled cold atoms in an optical lattice and spin-current generation *Phys. Rev. A* **99** 023604
- [43] Mossman M E, Hou J, Luo X-W, Zhang C and Engels P 2019 Experimental realization of a non-magnetic one-way spin switch *Nat. Commun.* **10** 3381
- [44] Wang C, Gao C, Jian C-M and Zhai H 2010 Spin-orbit coupled spinor Bose-Einstein condensates *Phys. Rev. Lett.* **105** 160403
- [45] Ho T-L and Zhang S 2011 Bose-Einstein condensates with spin-orbit interaction *Phys. Rev. Lett.* **107** 150403
- [46] Li Y, Pitaevskii L P and Stringari S 2012 Quantum tricriticality and phase transitions in spin-orbit

- coupled Bose-Einstein condensates *Phys. Rev. Lett.* **108** 225301
- [47] Zheng W, Yu Z-Q, Cui X and Zhai H 2013 Properties of Bose gases with the Raman-induced spin-orbit coupling *J. Phys. B At. Mol. Opt. Phys.* **46** 134007
 - [48] Juršėnas R and Ruseckas J 2013 Bound states of the spin-orbit coupled ultracold atom in a one-dimensional short-range potential *J. Math. Phys.* **54** 051901
 - [49] Kartashov Y V, Konotop V V and Torner L 2017 Bound states in the continuum in spin-orbit-coupled atomic systems *Phys. Rev. A* **96** 033619
 - [50] Kittel C 2005 *Introduction to solid state physics* (Wiley).
 - [51] Frost A A 1956 Delta-function model I: Electronic energies of Hydrogen-like atoms and diatomic molecules *J. Chem. Phys.* **25** 1150
 - [52] Huang K and Yang C N 1957 Quantum-mechanical many-body problem with hard-sphere interaction *Phys. Rev.* **105** 767
 - [53] Block M and Holthaus M 2002 Pseudopotential approximation in a harmonic trap *Phys. Rev. A* **65** 052102
 - [54] Uncu H, Tarhan D, Demiralp E, and Müstecaplıoğlu Ö E 2007 Bose-Einstein condensate in a harmonic trap decorated with Dirac δ functions *Phys. Rev. A* **76**, 013618
 - [55] Garrett M C, Ratnapala A, van Ooijen E D, Vale C J, Weegink K, Schnelle S K, Vainio O, Heckenberg N R, Rubinsztein-Dunlop H and Davis M J 2011 Growth dynamics of a Bose-Einstein condensate in a dimple trap without cooling *Phys. Rev. A* **83** 013630
 - [56] Łącki M, Baranov M A, Pichler H and Zoller P 2016 Nanoscale “dark state” optical potentials for cold atoms *Phys. Rev. Lett.* **117** 233001
 - [57] Wang Y, Subhankar S, Bienias P, Łącki M, Tsui T-C, Baranov M A, Gorshkov A V, Zoller P, Porto J V and Rolston S L 2018 Dark state optical lattice with a subwavelength spatial structure *Phys. Rev. Lett.* **120** 083601
 - [58] Hakim V 1997 Nonlinear Schrödinger flow past an obstacle in one dimension *Phys. Rev. E* **55** 2835
 - [59] Pavloff N 2002 Breakdown of superfluidity of an atom laser past an obstacle *Phys. Rev. A* **66** 013610
 - [60] Frantzeskakis D J, Theocharis G, Diakonov F K, Schmelcher P and Kivshar Y S 2002 Interaction of dark solitons with localized impurities in Bose-Einstein condensates *Phys. Rev. A* **66** 053608
 - [61] Seaman B T, Carr L D and Holland M J 2005 Effect of a potential step or impurity on the Bose-Einstein condensate mean field *Phys. Rev. A* **71** 033609
 - [62] Grimm R, Weidemüller M and Ovchinnikov Y B 2000 Optical Dipole Traps for Neutral Atoms *Adv. At. Mol. Opt. Phys.* **42** 95
 - [63] Sablikov V A and Tkach Y Y 2007 Evanescent states in two-dimensional electron systems with spin-orbit interaction and spin-dependent transmission through a barrier *Phys. Rev. B* **76** 245321
 - [64] Chin C, Grimm R, Julienne P and Tiesinga E 2010 Feshbach resonances in ultracold gases *Rev. Mod. Phys.* **82** 1225
 - [65] Timmermans E, Tommasini P, Hussein M and Kerman A 1999 Feshbach resonances in atomic Bose-Einstein condensates *Phys. Rep.* **315** 199
 - [66] Wu C 2009 Unconventional Bose-Einstein condensations beyond the “no-node” theorem *Mod. Phys. Lett. B* **23** 1
 - [67] Zhou X, Li Y, Cai Z and Wu C 2013 Unconventional states of bosons with the synthetic spin-orbit coupling *J. Phys. B At. Mol. Opt. Phys.* **46** 134001
 - [68] Hsu C W, Zhen B, Stone A D, Joannopoulos J D and Soljačić M 2016 Bound states in the continuum *Nat. Rev. Mater.* **1** 16048